

The effect of turbulent pressure on the red giants and AGB stars

I. On the internal structure and evolution

S.Y. Jiang and R.Q. Huang

Yunnan observatory, Chinese Academy of Sciences, P.O. Box 110, 650011 Kunming, P.R. China

Received 24 January 1996 / Accepted 7 May 1996

Abstract. The expressions for the turbulent pressure, equation of state and thermodynamic quantities taking account of turbulent pressure are derived in the framework of the mixing-length theory of convection. The numerical computations indicate that the turbulent pressure in the region close to the surface of a red giant or an AGB star can reach a value of 30–40 percent of the total pressure. A comparison of the evolution of a star with $7M_{\odot}$ from the zero-age main sequence to the AGB stage adopting turbulent pressure with that of the neglected turbulent pressure shows that the effect of turbulent pressure on the internal structure and evolution in the phase from the He-core burning stage to the AGB stage is significant. A similar investigation for the star of $2.8M_{\odot}$ shows that the effect of turbulent pressure on the internal structure in the same evolutionary phase is small. However, the effect of turbulent pressure on the evolutionary track in the AGB phase is obvious.

Key words: stars: AGB – stars: interiors – stars: evolution – convection – turbulence

1. Introduction

The contribution of turbulent pressure is generally neglected in the investigations of the structure and evolution of low and intermediate massive stars. However, when the stars evolve to the red giant stage and the AGB stage, their envelopes are totally convective, and the energy transported by convection is much greater than that transported by radiation. Therefore the turbulent pressure may be important in the envelopes of red giants and AGB stars. The purpose of this paper is to give the expressions for the turbulent pressure, equation of state and thermodynamic quantities taking account of turbulent pressure based on the mixing-length theory, and to investigate the effect of the turbulent pressure on the internal structure and evolution of red giants and AGB stars.

Send offprint requests to: R.Q. Huang

2. Basic equations

Convective flows in stars are complex turbulent motions. A thorough theoretical treatment of convection must be based on a theory of turbulent motions and is extremely difficult. Although there have been several theories of convection based on analytic approaches to the basic fluidodynamic equations in the last years (cf. Xiong, 1977, 1979, 1981; Canuto & Mazzitelli, 1991, 1992; Canuto, 1992), none of them, however, has reached a stage where it can provide a procedure easy enough to be handled in stellar structure calculations. The following derivations of the expressions for the turbulent pressure, equation of state and thermodynamic quantities taking account of turbulent pressure have, therefore, to be based on the mixing-length theory, and have approximate character.

2.1. Turbulent pressure

The turbulent pressure P_t is a function of the density ρ and the velocity \bar{v} of the average convective element, and is expressed as:

$$P_t = Q\rho\bar{v}^2, \quad (1)$$

where Q is a coefficient of order unity. Here, we put $Q = 1$ according to Henyey et al. (1965) and de Jager (1980). The average velocity \bar{v} is obtained by solving the equations of the mixing-length theory (see Hofmeister et al., 1964) and can be expressed as

$$\bar{v}^2 = \frac{\alpha_l^2 \delta P}{8\rho} \left(W - \frac{8}{27}U - \frac{E}{3} \frac{1}{W} \right)^2, \quad (2)$$

where

$$W = \left(\frac{A}{2} + \sqrt{D} \right)^{1/3},$$

$$D = \left(\frac{A}{2} \right)^2 + \left(\frac{E}{3} \right)^3,$$

$$\frac{E}{3} = \frac{368}{729} U^2, \quad (3)$$

$$\frac{A}{2} = \left[\frac{4}{9}(\nabla_r - \nabla_{ad}) + \left(\frac{19^3}{27^3} - \frac{1}{9} \right) U^2 \right] U,$$

$$U = \frac{3acT^3}{C_p \rho^2 l \bar{\kappa}} \left(\frac{8H_p}{gl^2 \delta} \right)^{1/2},$$

$$l = \alpha_l H_p.$$

l , H_p , C_p and $\bar{\kappa}$ are the mixing length, the pressure scale height, the specific heat at constant pressure and the opacity, respectively. ∇_{ad} and ∇_r are the adiabatic and radiation temperature gradients. $\delta \equiv -\left(\frac{\partial \ln \rho}{\partial \ln T}\right)_p$.

2.2. The equation of state and the thermodynamic quantities adopting the turbulent pressure

The total pressure P at a given point in the convective envelope consists of the radiation pressure P_r , turbulent pressure P_t and gas pressure P_g , which is the sum of the partial pressure of free electrons P_e and the partial pressure of nuclei P_i :

$$P = P_r + P_t + P_g = P_r + P_t + P_e + P_i. \quad (4)$$

We introduce two dimensionless quantities:

$$\beta_t = \frac{P_t}{P} \quad (5)$$

and

$$\beta = \frac{P_t + P_g}{P}. \quad (6)$$

Using (1),(2) and (5), we have

$$\beta_t = \frac{\alpha_l^2 \delta}{8} \left(W - \frac{8}{27} U - \frac{E}{3} \frac{1}{W} \right)^2. \quad (7)$$

From (4),(6) and $P_r = \frac{a}{3} T^4$, we obtain

$$\beta = 1 - \frac{aT^4}{3P}. \quad (8)$$

The thermodynamic properties of stellar material depend on its degree of ionization. In the following we derive the equation of state and some thermodynamic quantities for the cases of complete and partial ionization, respectively: A. The case of complete ionization

Using Eqs. (1),(4),(5),(8) and the relations $P_g = \frac{\mathcal{R}}{\mu} \rho T$, $P_e = \frac{\mathcal{R}}{\mu_e} \rho T$ and $P_i = \frac{\mathcal{R}}{\mu_i} \rho T$, we obtain the equation of state for the case of complete ionization as

$$\rho = \frac{\mu}{\mathcal{R} T} (\beta - \beta_t), \quad (9)$$

where \mathcal{R} is the gas constant; μ , μ_e and μ_i are the mean molecular weights for free particles, free electrons and nuclei, respectively.

In the case of complete ionization the inner energy per gram of material consists of the kinetic energy of particles, the radiation energy and the turbulent energy:

$$U = \frac{3}{2} \frac{\mathcal{R}}{\mu} T + U_r + U_t. \quad (10)$$

Setting $U_r = \frac{aT^4}{\rho} = \frac{3P_r}{\rho} = 3(1 - \beta) \frac{P}{\rho}$ and $U_t = 3\bar{v}^2 = \frac{3P_t}{\rho}$ into (10), we obtain

$$U = \frac{3}{2} (2 - \beta + \beta_t) \frac{P}{\rho}. \quad (11)$$

The specific heat at constant pressure C_p and the adiabatic temperature gradient ∇_{ad} for the case of complete ionization can be written as

$$C_p = \left(\frac{\partial U}{\partial T} \right)_p + \frac{P}{\rho T} \delta = \frac{P}{\rho T} \left[\left(4 - \frac{3}{2} \beta + \frac{3}{2} \beta_t \right) \delta + 6(1 - \beta) + \frac{3}{2} \left(\frac{\partial \beta_t}{\partial \ln T} \right)_p \right] \quad (12)$$

and

$$\nabla_{ad} = \left(\frac{d \ln T}{d \ln P} \right)_{ad} = \frac{P \delta}{C_p T \rho}. \quad (13)$$

B. The case of partial ionization

In the case of partial ionization the pressure of free electrons P_e is written as

$$P_e = \frac{\mathcal{R} E'}{\mu_i} \rho T, \quad (14)$$

where E' gives the number of free electrons per atom. The total pressure can be expressed as

$$P = \frac{\mathcal{R}}{\mu_i} (1 + E') \rho T + \frac{a}{3} T^4 + \rho \bar{v}^2. \quad (15)$$

The equation of state for the case of partial ionization can be obtained as

$$\rho = \frac{\mu'}{\mathcal{R} T} (\beta - \beta_t), \quad (16)$$

where

$$\mu' = \frac{\mu_i}{1 + E'}. \quad (17)$$

In the case of partial ionization the inner energy per gram of material consists of the kinetic energy of particles, the radiation energy, the turbulent energy and the ionization energy:

$$U = \frac{3}{2} \frac{\mathcal{R}}{\mu} T + U_r + U_t + U_i. \quad (18)$$

The ionization energy for a gas of hydrogen and helium is written as

$$U_i = \frac{\mathcal{R}}{\mu_i k} \left[\nu_H \eta_H \chi_H + \nu_{He} (\eta_{He} + \eta_{He^+}) \chi_{He} + \nu_{He} \eta_{He^+} \chi_{He^+} \right], \quad (19)$$

where χ_H denotes the ionization energy of hydrogen. χ_{He} and χ_{He^+} are the ionization energy for neutral and single ionized helium. η_H , η_{He} and η_{He^+} denote the degrees of ionizations for hydrogen and helium respectively. $\nu_H = \frac{4X}{4X+Y}$ and $\nu_{He} = \frac{Y}{4X+Y}$ denote the weight fractions of hydrogen and helium in a gram of

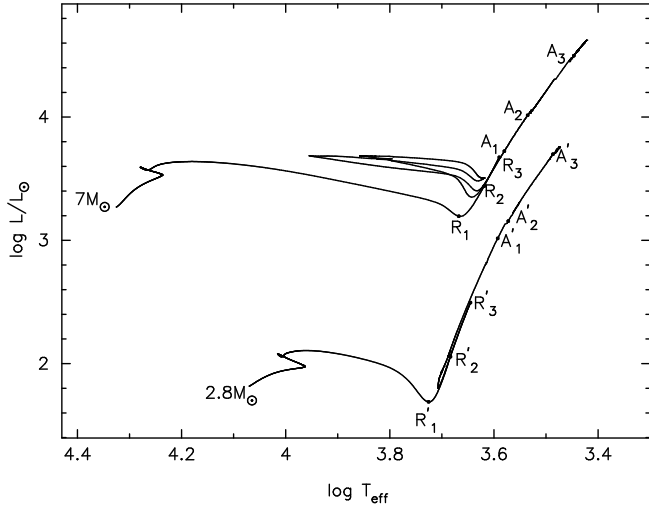


Fig. 1. The HR diagram with evolutionary tracks from the zero-age main sequence to the AGB stage for stars with masses of $7M_{\odot}$ and $2.8M_{\odot}$ and with an initial composition of $X = 0.68$, $Y = 0.30$. The letters A_1, A_2, A_3 , and A'_1, A'_2, A'_3 denote different evolutionary times in the AGB stage, while the letters R_1, R_2, R_3 , and R'_1, R'_2, R'_3 , denote those in the giant branch stage.

mixture, respectively. X and Y are the mass fractions of hydrogen and helium.

For a mixture of hydrogen-helium gas the specific heat at constant pressure C_p and the adiabatic temperature gradient ∇_{ad} for the case of partial ionization are expressed as

$$C_p = \frac{P}{\rho T} \left[\left(4 - \frac{3}{2}\beta + \frac{3}{2}\beta_t\right)(\delta + \mu'_T) + 6(1 - \beta) - 4\mu'_T\beta_t \right. \\ \left. + \left(\frac{3}{2} + \mu'_T\right) \left(\frac{\partial\beta_t}{\partial\ln T}\right)_p \right] + \frac{P}{\rho T} \frac{(\beta - \beta_t)}{(1 + E')} \left(\frac{\nu_H}{G_H} \phi_H^2 \right. \\ \left. + \frac{\nu_{He}}{G_{He}} \phi_{He}^2 + \frac{\nu_{He^+}}{G_{He^+}} \phi_{He^+}^2 \right), \quad (20)$$

and

$$\nabla_{ad} = \frac{\delta P}{C_p \rho T}, \quad (21)$$

where

$$\mu'_T \equiv \left(\frac{\partial\ln\mu'}{\partial\ln T}\right)_p \\ = -\frac{1}{1 + E'} \left(\frac{\nu_H}{G_H} \phi_H + \frac{\nu_{He}}{G_{He}} \phi_{He} + \frac{\nu_{He^+}}{G_{He^+}} \phi_{He^+} \right), \\ \phi_H = A + \frac{\chi_H}{kT}, \quad \phi_{He} = A + \frac{\chi_{He}}{kT}, \\ \phi_{He^+} = A + \frac{\chi_{He^+}}{kT}, \quad (22) \\ A = \frac{5}{2} + \frac{4(1 - \beta) + \left(\frac{\partial\beta_t}{\partial\ln T}\right)_p}{\beta - \beta_t}, \\ \frac{\nu_H}{G_H} = \frac{\nu_H \eta_H (1 - \eta_H)}{1 + \frac{\nu_H \eta_H (1 - \eta_H)}{E'(1 + E')}},$$

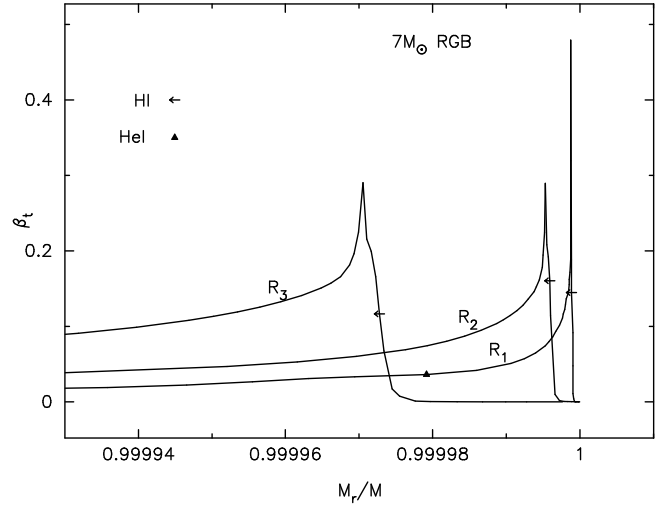


Fig. 2. The variation of the ratio β_t of the turbulent pressure to the total pressure in the envelope of the $7M_{\odot}$ star in the giant branch phase. The labels R_1, R_2 and R_3 have the same meaning as shown in Fig. 1. The arrows denote the hydrogen ionization regions.

$$\frac{\nu_{He}}{G_{He}} = \frac{\nu_{He}(\eta_{He} + \eta_{He^+})(1 - \eta_{He} - \eta_{He^+})}{1 + \frac{\nu_{He}(\eta_{He} + \eta_{He^+})(1 - \eta_{He} - \eta_{He^+})}{E'(1 + E')}}}, \\ \frac{\nu_{He}}{G_{He^+}} = \frac{\nu_{He} \eta_{He^+} (1 - \eta_{He^+})}{1 + \frac{\nu_{He} \eta_{He^+} (1 - \eta_{He^+})}{E'(1 + E')}}}.$$

3. The effect of turbulent pressure on the structure and evolution

In order to know the effect of turbulent pressure on the internal structure and evolution of red giants and AGB stars, we computed the evolution for stars with initial masses of $7M_{\odot}$ and $2.8M_{\odot}$ from the main sequence to the AGB stage including or neglecting the turbulent pressure.

3.1. Numerical model

The structure and evolution of stars are followed with a modified version of a stellar structure program developed by Kippenhahn et al. (1967) and updated to include the revised opacities (cf. Rogers & Iglesias 1992; Li 1994) and the most recent nuclear reaction rates (cf. Maeder 1983; Maeder and Meynet 1987, 1989). The turbulent pressure, equation of state and thermodynamic quantities involving the turbulent pressure are given by the formulae in Sect. 2. The chemical compositions of the stars of $7M_{\odot}$ and $2.8M_{\odot}$ are $X = 0.68$ and $Z = 0.02$. The mass loss rate (in $M_{\odot} \text{ yr}^{-1}$) is from Reimers (1975):

$$\dot{M} = -4 \times 10^{-13} \eta \frac{LR}{M}, \quad (23)$$

where L, R and M are given in solar units and the value of η is taken to be 0.7 for the low and intermediate massive stars (cf. Maeder & Meynet 1989).

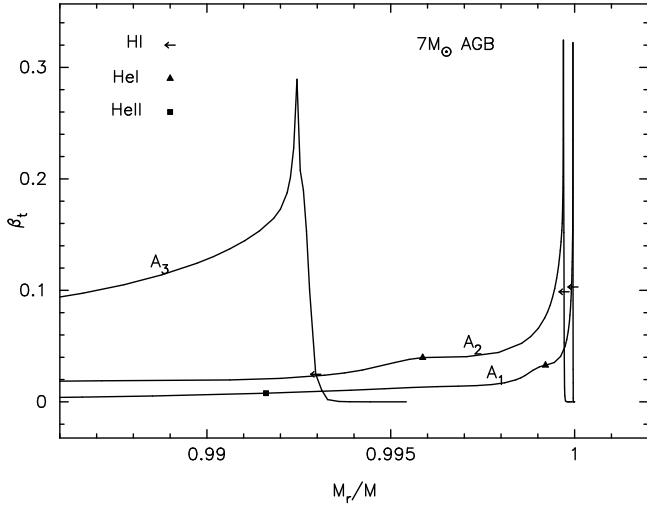


Fig. 3. The variation of the ratio β_t of the turbulent pressure to the total pressure in the envelope of the $7M_{\odot}$ star in the AGB stage. The labels A_1 , A_2 , and A_3 have the same meaning as shown in Fig. 1. The arrows denote the hydrogen ionization regions.

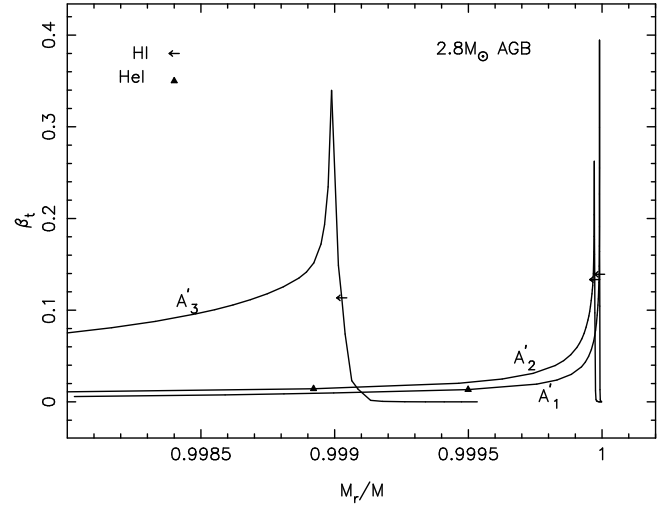


Fig. 5. The variation of the ratio β_t of the turbulent pressure to the total pressure in the envelope of the $2.8M_{\odot}$ star in the AGB stage. The letters A'_1 , A'_2 and A'_3 have the same meaning as shown in Fig. 1. The arrows show the hydrogen ionization regions.

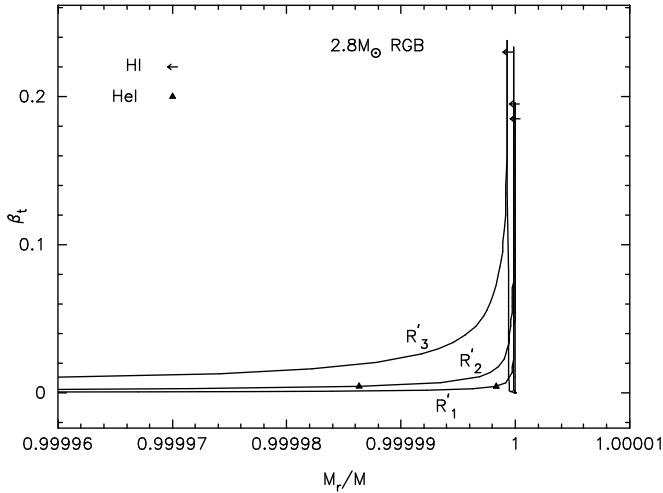


Fig. 4. The variation of the ratio β_t of the turbulent pressure to the total pressure in the envelope of the $2.8M_{\odot}$ star in the giant branch stage. The letters R'_1 , R'_2 and R'_3 have the same meaning as shown in Fig. 1. The arrows show the hydrogen ionization regions.

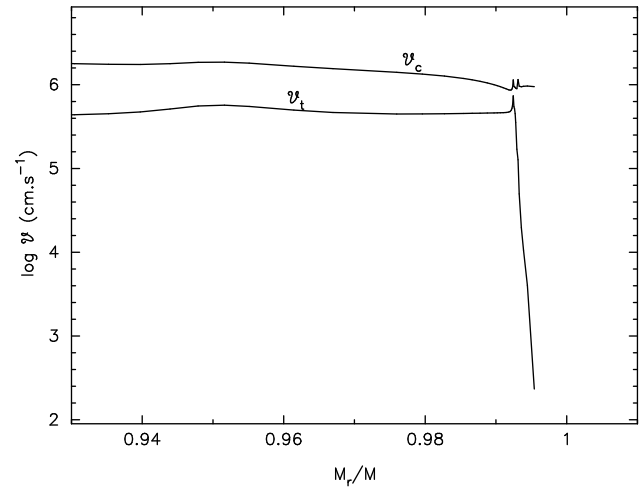


Fig. 6. The changes in the turbulent velocity v_t and the sound-speed v_c in the envelope of the AGB star of $7M_{\odot}$.

3.2. Results

The evolution of stars with masses of $7M_{\odot}$ and $2.8M_{\odot}$ is illustrated in the HR diagram of Fig. 1. Along the evolutionary track of the $7M_{\odot}$ star the points marked with R_1 , R_2 and R_3 , and the points labelled as A_1 , A_2 and A_3 mark different evolutionary times in the red giant stage and the AGB stage, respectively. Similar points along the track of the $2.8M_{\odot}$ star are labelled with R'_1 , R'_2 and R'_3 , and with A'_1 , A'_2 , A'_3 . The radial profiles of the ratio β_t of the turbulent pressure to the total pressure in the envelopes of the $7M_{\odot}$ star during the red giant stage and the AGB stage are illustrated in Figs. 2 and 3, in which the labels R_1 , R_2 , R_3 , A_1 , A_2 and A_3 , and R'_1 , R'_2 , R'_3 , A'_1 , A'_2 and A'_3 , have the

same meaning as shown in Fig. 1. The arrows in both Figs. 2 and 3 denote the hydrogen ionization regions. From Figs. 2 and 3 we find that the turbulent pressures always have a maximal value of 30-40 percent of the total pressure in the hydrogen ionization regions, which are very close to the surfaces of these stars. The radiation pressures in the same regions is, however, only 0.3-0.6 percent of the total pressure. The difference between Fig. 2 and Fig. 3 is that the positions of the maximal values of turbulent pressure for AGB stars are slightly deeper in the envelopes than that for red giants. Figs. 4 and 5 show the radial profiles of the ratio β_t of the turbulent pressure to the total pressure in the envelopes of the $2.8M_{\odot}$ star in the red giant stage and in the AGB stage. They have the same properties as shown in Figs. 2 and 3.

Canuto and Mazzitelli (1991) studied the turbulent pressure for the stars of low mass based on their model for large scale

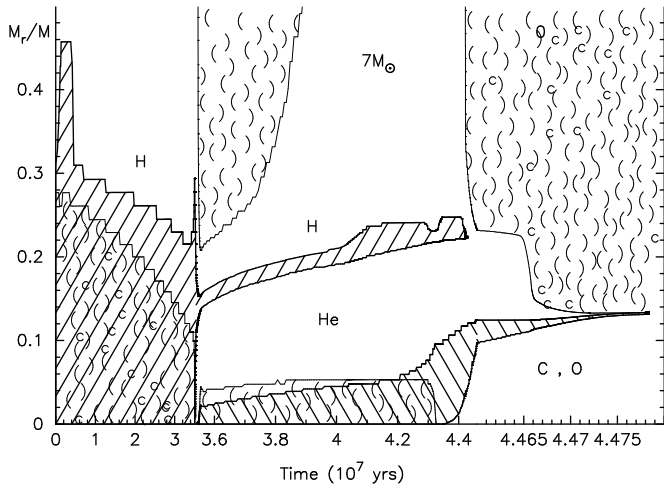


Fig. 7. The evolution of the internal structure of a star of $7M_{\odot}$ with the initial composition $X = 0.68$ and $Z = 0.02$ taking account of turbulent pressure. The “Cloudy” regions indicate convective areas. The main regions of nuclear burning are heavily hatched. The region where the nuclear energy generation rate of hydrogen exceeds $10 \text{ erg g}^{-1} \text{ s}^{-1}$ is dotted.

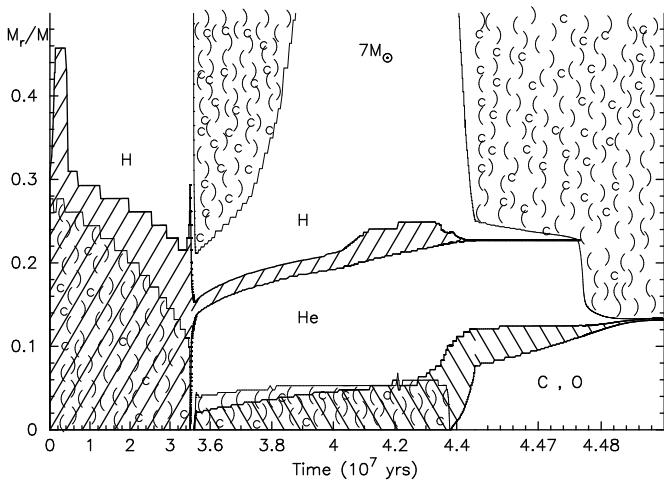


Fig. 8. The evolution of the internal structure of the star of $7M_{\odot}$ without consideration of turbulent pressure is plotted in the same manner as in Fig. 7.

turbulent convection. Their computations indicate that, in the case of the sun, the turbulent pressure can easily reach 10% of the total pressure, while for red giants it can be as large as 40% – 50%.

Fig. 6 illustrates the changes in the turbulent velocity v_t and the sound-speed v_c in the entire envelope of the AGB star of $7M_{\odot}$. From Fig. 6 it can be seen that the turbulent velocity keeps subsonic in the total envelope, and the gradient of the turbulent velocity keeps small in the envelope except for the region close to the surface, where the turbulent velocity reaches a maximum value and then falls down rapidly. Canuto(1991) pointed out that the turbulent flux should be the flux of mixing-length theory corrected by adding a diffusion term in the region with a

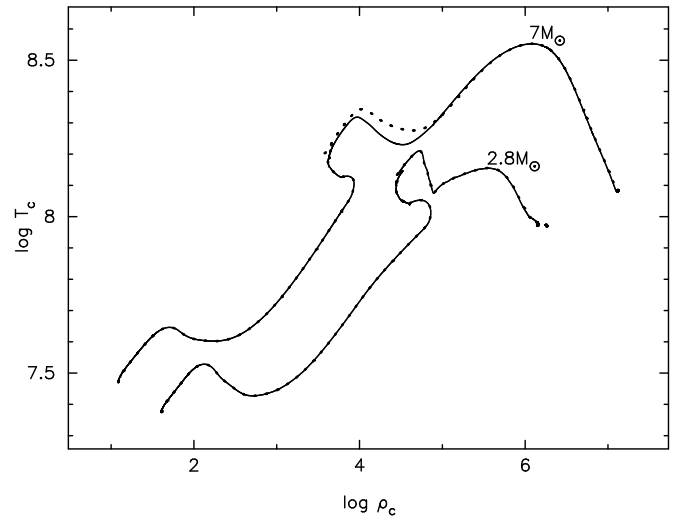


Fig. 9. The central temperature T_c (in $^{\circ}\text{K}$) is plotted over the central density ρ_c (in g cm^{-3}) for the stars of $7M_{\odot}$ and $2.8M_{\odot}$. The solid and dotted curves indicate the cases with and without the contribution of turbulent pressure, respectively.

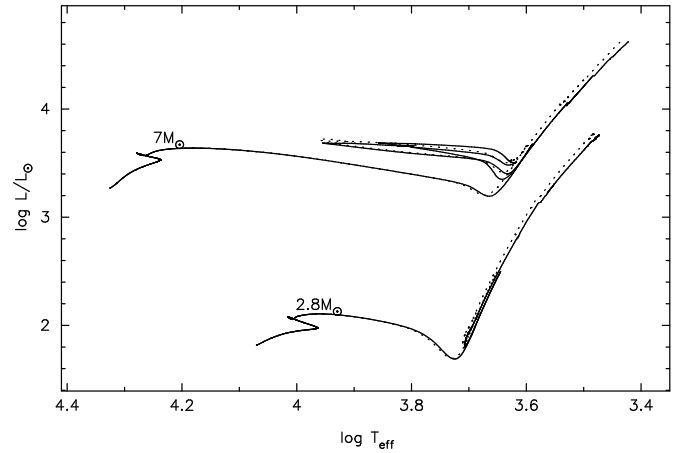


Fig. 10. The HR diagram with evolutionary tracks of the stars with masses of $7M_{\odot}$ and $2.8M_{\odot}$. The solid and dotted curves indicate the cases with and without the consideration of turbulent pressure, respectively.

large gradient of turbulent velocity. This means that the turbulent velocity should be greater than that given in Fig. 6 in the region close to the surface of the star.

The evolution of the internal structure for the star with $7M_{\odot}$ from the zero-age main sequence to the early AGB stage with the inclusion of turbulent pressure is illustrated in Fig. 7, while the evolution of the internal structure for the same star neglecting turbulent pressure is illustrated in Fig. 8. We find that the H-burning shell in Fig. 7 is thicker and vanishes earlier than that in Fig. 8. This indicates that owing to the effect of turbulent pressure the H-burning shell becomes thicker and vanishes earlier for the star with $7M_{\odot}$ in the evolutionary phase from the He-core burning stage to the early AGB stage. Concerning the evolution of the internal structure for the star of $2.8M_{\odot}$

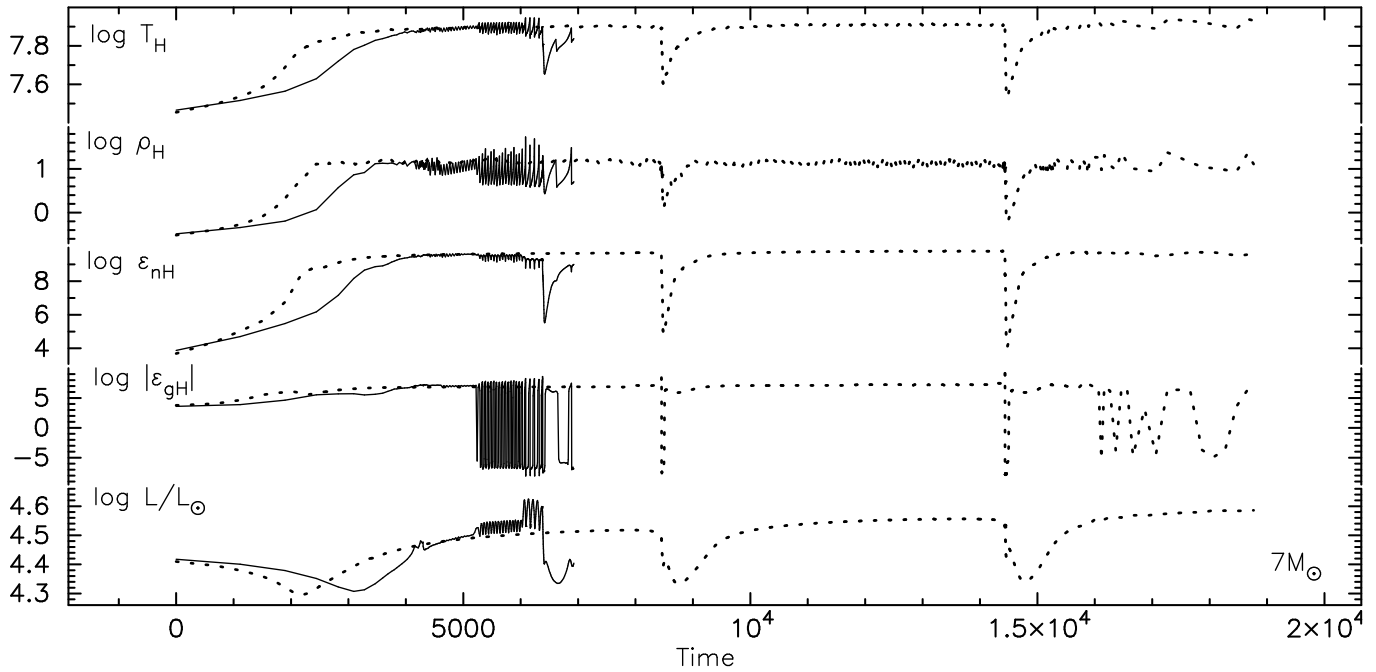


Fig. 11. The changes in the temperature, density, nuclear energy generation rate and thermal generation rate of the H-burning shell, and the variation of the luminosity of the star with $7M_{\odot}$ during the thermal pulses AGB stage. The solid and dotted curves indicate the cases with and without the consideration of turbulent pressure, respectively.

adopting or neglecting turbulent pressure, we find no appreciable differences. The variations of the central temperature versus the central density for the stars with masses of $7M_{\odot}$ and $2.8M_{\odot}$ are illustrated in Fig. 9. The solid curves and the dotted curves in Fig. 9 (also in all of the following figures) correspond to the cases with and without the consideration of turbulent pressure respectively. From this figure one finds that the central temperature for the star of $7M_{\odot}$ during the He-core burning phase adopting turbulent pressure becomes lower than that neglecting turbulent pressure. However, there is no difference between the curves in Fig. 9 for the star of $2.8M_{\odot}$. The evolutionary tracks in the HR diagram from the zero-age main sequence to the AGB stage for the stars with masses of $7M_{\odot}$ and $2.8M_{\odot}$ are illustrated in Fig. 10. From which we see that the effect of turbulent pressure makes the evolutionary track of $7M_{\odot}$ move into the region of higher luminosity during the He-core burning stage, and move into the region of lower temperature during the early AGB stage. The changes in the evolutionary track can be understood by the fact that owing to the effect of turbulent pressure the H-burning shell, which is the main energy source of the $7M_{\odot}$ star, becomes thicker in the He-core burning stage and vanishes earlier in the early AGB stage. In Fig. 10 one sees that the track of the star with $2.8M_{\odot}$ also moves into the region of lower temperature in the early AGB stage.

We also investigated the effect of turbulent pressure on the thermal pulses in the AGB stage. Fig. 11 shows the evolution of the temperature T_H , density ρ_H , nuclear energy generation rate ϵ_{nH} and thermal energy generation rate ϵ_{gH} of the H-burning shell for the star of $7M_{\odot}$. The evolution of the luminosity of the $7M_{\odot}$ star during the same stage is also illustrated in Fig. 11, where

many pulsations can be found from the curves taking account of turbulent pressure, but no pulsation can be found from the dotted curves. This means that the effect of turbulent pressure causes the occurrence of pulsations in the H-burning shell for the star of $7M_{\odot}$. In Fig. 11 we also find pulsations in the luminosity curve for the star of $7M_{\odot}$, which indicates that the luminosity of the star comes mainly from the luminosity of the H-burning shell. Fig. 12 is an enlargement of Fig. 11. From Fig. 12 we obtain for the average period of the pulsations of the H-burning shell about 50 years. The variations versus time for the temperature, nuclear energy generation rate and density of the He-burning shell of the $7M_{\odot}$ star are illustrated in Fig. 13. Comparing the solid curves with the dotted curves in Fig. 13, one finds that the effect of turbulent pressure causes the earlier occurrence of the thermal pulses of the He-burning shell and the shortening of the period of the thermal pulses. Concerning the thermal pulses in the AGB stage for the star with $2.8M_{\odot}$ adopting or neglecting turbulent pressure, we find no appreciable differences.

4. Summary

Owing to the effect of turbulent pressure the H-burning shell of the $7M_{\odot}$ star becomes thicker and vanishes earlier in the period from the He-core burning stage to the early AGB stage. The corresponding evolutionary track in the HR diagram moves into the region of higher luminosity during the He-core burning stage, and into the region of lower temperature during the early AGB stage. In the thermal pulses AGB stage of the star with $7M_{\odot}$ the effect of turbulent pressure causes the occurrence of

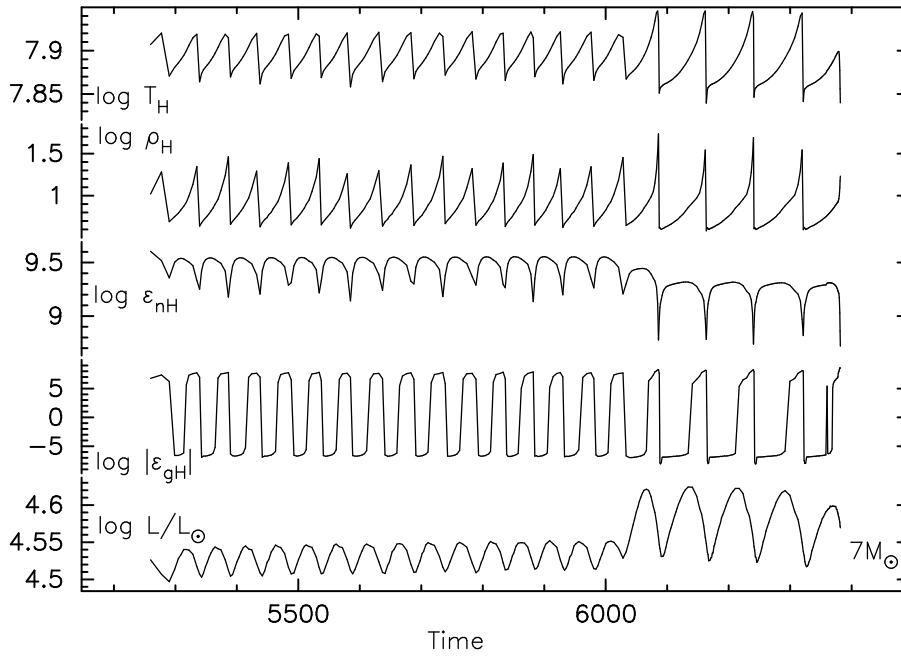


Fig. 12. The enlargement of Fig. 11.

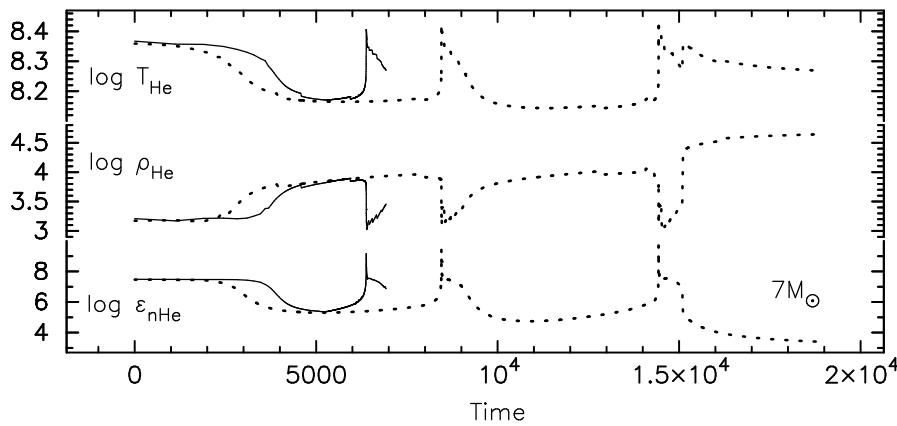


Fig. 13. The changes in the temperature, density and energy generation rate of the He-burning shell of the $7M_{\odot}$ star during the thermal pulse AGB stage. The solid and dotted curves indicate the cases with and without the consideration of turbulent pressure, respectively.

pulsations with a period of 50 years for the H-burning shell. In addition, this effect causes the earlier occurrence of the thermal pulses of the He-shell and the shortening of its period.

The effect of turbulent pressure on the internal structure of the star with $2.8M_{\odot}$ is weak. However, its evolutionary track in the HR diagram moves into the region of lower temperature during the early AGB phase owing to the effect of turbulent pressure.

Acknowledgements. The authors gratefully acknowledge Dr. P. Bernasconi for comments and suggestions on this paper. This research is supported by the National Natural Science Foundation of China.

References

- Canuto V.M., Mazzitelli I., 1991, ApJ 370, 295
 Canuto V.M., Mazzitelli I., 1992, ApJ 389, 724
 Heneyey L.G., Vardya M.S., Bodenheimer P.L., 1965, ApJ 142, 841
 Hofmeister E., Kippenhahn R., Weigert A., 1964, Z.Ap. 59, 215
 De Jager C., 1980, The Brightest Stars, Reidel, Dordrecht
 Kippenhahn R., Weigert A., Hofmeister E., 1967, Method in Computational Physics, Vol.7, Academy Press, New York, p. 129
 Li Y., 1994, A&A 286, 815
 Maeder A., 1983, A&A 120, 113
 Maeder A., Meynet G., 1987, A&A 182, 243
 Maeder A., Meynet G., 1989, A&A 210, 155
 Reimers D., 1975, Mem.Soc.R.Sci.Liege, 6 Ser.8, 369
 Rogers, F.J., Iglesias, C.A., 1992, ApJS 79, 507
 Xiong D.R., 1977, Acta Astron.Sinica 20, 3, 238
 Xiong D.R., 1979, Acta Astron. Sinica 18, 1, 86
 Xiong D.R., 1981, Science in China 6, 705